

SCIENTIFIC REPORTS



OPEN

Dual mTOR/PI3K inhibition limits PI3K-dependent pathways activated upon mTOR inhibition in autosomal dominant polycystic kidney disease

Yang Liu^{1,10}, Martin Pejchinovski², Xueqi Wang³, Xuebin Fu⁴, Deborah Castelletti⁵, Terry J. Watnick⁶, Alexandre Arcaro⁷, Justyna Siwy², William Mullen⁸, Harald Mischak^{2,8} & Andreas L. Serra⁹

Autosomal dominant polycystic kidney disease (ADPKD) is characterized by the development of kidney cysts leading to kidney failure in adulthood. Inhibition of mammalian target of rapamycin (mTOR) slows polycystic kidney disease (PKD) progression in animal models, but randomized controlled trials failed to prove efficacy of mTOR inhibitor treatment. Here, we demonstrate that treatment with mTOR inhibitors result in the removal of negative feedback loops and up-regulates pro-proliferative phosphatidylinositol 3-kinase (PI3K)-Akt and PI3K-extracellular signal-regulated kinase (ERK) signaling in rat and mouse PKD models. Dual mTOR/PI3K inhibition with NVP-BEZ235 abrogated these pro-proliferative signals and normalized kidney morphology and function by blocking proliferation and fibrosis. Our findings suggest that multi-target PI3K/mTOR inhibition may represent a potential treatment for ADPKD.

Autosomal dominant polycystic kidney disease (ADPKD) is the most common potentially lethal monogenetic hereditary kidney disease. It is characterized by progressive dilation of renal tubules that eventually form cysts, leading to kidney failure¹. The loss of the major function of the kidneys due to cysts expansion has been largely associated with unexpected or asymptomatic well-know germ-line mutations, somatic mutations or even by reperfusion processes of ischemic tissue. These adverse effects are followed by glomerular hyperfiltration as a result of excess fluid accumulation^{1,2}.

One of the key components is the mammalian target of rapamycin (mTOR) kinase which is a master regulator of protein synthesis and proliferation aberrantly activated during ADPKD onset^{2,3}. Although treatment with mTOR inhibitors has shown positive results in preventing massive renal enlargement in a variety of polycystic kidney disease (PKD) animal models, clinical trials have not been able to show the same beneficial effect of mTOR inhibitors treatment in ADPKD patients⁴⁻⁸. It could be argued that a lack of good experimental study design, inappropriate drug dosage, inadequate therapy duration or patient stratification could be the reasons for such poor clinical outcomes. However, several studies investigated the dual negative feedback loop in a variety of human cancers: mTOR/S6K activation attenuates upstream phosphatidylinositol 3-kinase (PI3K) pathway

¹Institute of Physiology, University of Zürich, Zürich, Switzerland. ²Mosaiques Diagnostics GmbH, Hanover, Germany. ³Department of Nephrology, Second Military Medical University, Shanghai, China. ⁴Department of Chemistry and Applied Biosciences, Molecular Pharmacology Unit, Swiss Federal Institute of Technology Zürich, Zürich, Switzerland. ⁵Novartis Institute for Biomedical Research, Basel, Switzerland. ⁶Division of Nephrology, University of Maryland School of Medicine, Baltimore, Maryland, United States of America. ⁷Department of Clinical Research, University of Bern, Bern, Switzerland. ⁸Institute of Cardiovascular and Medical Sciences, University of Glasgow, Glasgow, UK. ⁹Epidemiology, Biostatistics and Prevention Institute, University of Zürich, and Suisse ADPKD, Klinik Hirslanden Zürich, Switzerland. ¹⁰Present address: Department of Biomedicine, Cancer Immunology Laboratory, University Hospital Basel, Basel, Switzerland. Yang Liu and Martin Pejchinovski contributed equally to this work. Correspondence and requests for materials should be addressed to A.L.S. (email: andreas.serra@uzh.ch)

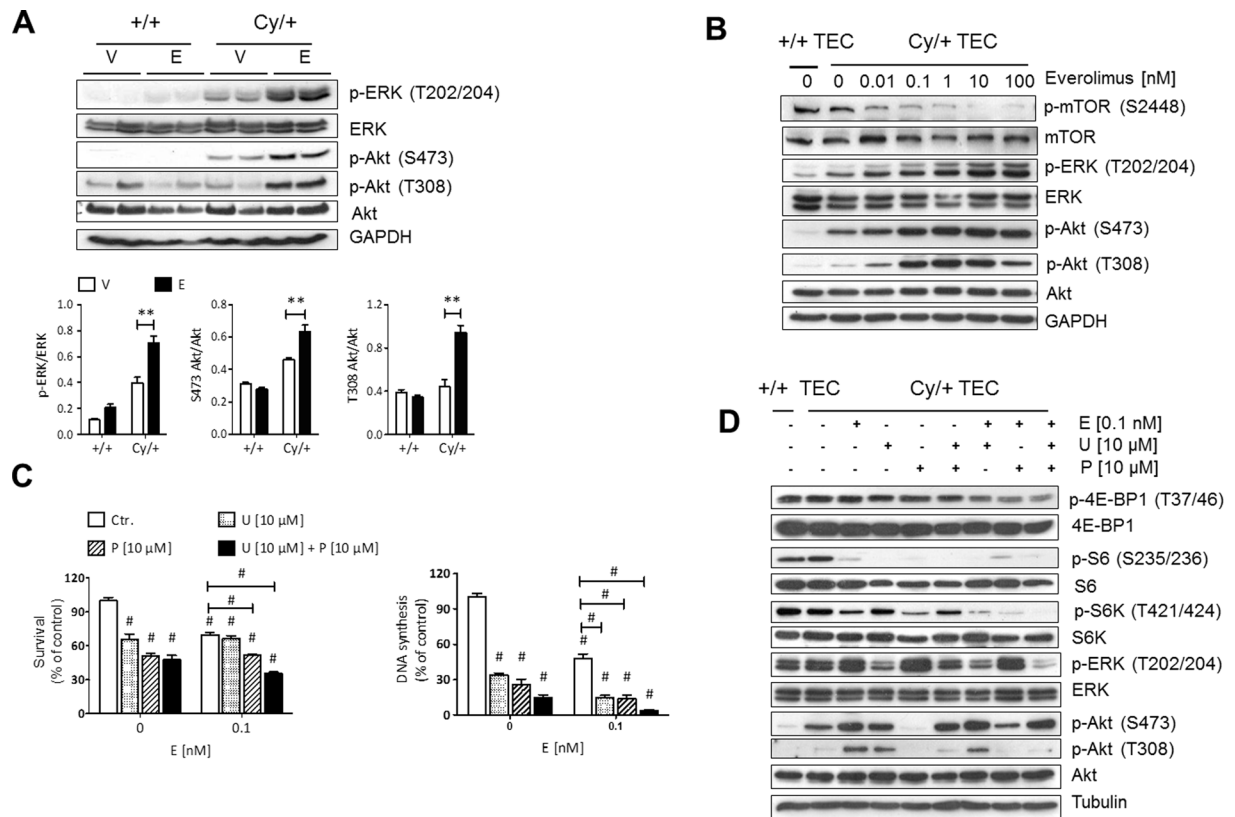


Figure 1. Mammalian TOR pathway blockage triggered dual PI3K-dependent feedback loops stemming from S6K to PI3K/ERK and to PI3K/Akt in PKD. **(A)** Han:SPRD rats whole kidney lysates western blot analysis and densitometry of PI3K/Akt and PI3K/ERK pathway readouts after 12 weeks everolimus (E) or vehicle (V) treatment ($n = 4$ per group). $**p < 0.01$ indicated by brackets. **(B)** mTOR upon treatment with indicated everolimus concentration for 48 h. **(C)** Cell viability (MTS, left panel) and DNA synthesis (BrdU, right panel) of *Cy/+* renal primary tubular epithelial cells (TEC) after combined application of mTOR (everolimus, E), Akt (UO126, U) and ERK (perifosine, P) inhibitors for 48 h. $\#p < 0.001$ compared to control, except where indicated by brackets. **(D)** Western blot analysis of mTOR, PI3K/Akt and PI3K/ERK pathways after 48 h combination treatment with the indicated inhibitors in *Cy/+* TEC. Graphs are representative of three independent experiments. These are cropped gels and the original gels are presented in Supplementary Fig. 6.

activation, while treatment with mTOR inhibitors (rapamycin and its analogs) lead to a hyperactive insulin receptor substrate 1 (IRS-1)/PI3K pathway. This, in turn, increases the signaling toward the pro-proliferative extracellular signal-regulated kinases (ERK) and Akt pathways^{9–12}. Based on these findings and our previous experimental work, we hypothesized that mTOR inhibition might also lead to compensatory up-regulation of the PI3K-dependent pathway in ADPKD by the release of mTOR controlled negative feedback loops that may attenuate the efficacy of mTOR inhibitors.

Results and Discussion

To explore our hypothesis we examined the effect of mTOR inhibitors on these dual negative feedback loops *in vitro* and in an animal model of PKD. For this purpose, we first treated Han:SPRD male rats, a well characterized strain (*Cy/+*) that resembles human ADPKD, with the rapamycin analog everolimus (gavage 3 mg/kg/day) from 4 to 16 weeks of age^{8,13,14}. As a result, treatment with everolimus increased the activity of readouts of PI3K/Akt and PI3K/ERK in the polycystic kidney (Fig. 1A). Phosphorylation of T202/204-ERK, T308-Akt and S473-Akt were increased in polycystic kidneys of *Cy/+* animals whereas in *wild type* animals these pathways were not activated by everolimus. In our next *in vitro analysis*, cultured Han:SPRD *Cy/+* male renal tubular epithelial cells (TEC) were further investigated by everolimus treatment. This resulted in increased Akt and ERK activation and decreased activity of mTOR (phosphorylation of T389-S6K, T421/S424-S6K, S235/236-S6 and S240/244-S6, respectively) when used in a dose-dependent manner (Fig. 1B and D).

Previously although applying different methodology, Belibi and her colleagues carried out a similar study to determine the effect of rapamycin on PKD and the influence of the drug evaluation throughout alternation of pro-proliferative mammalian target of rapamycin complexes (mTORC1 and mTORC2) in female Han:SPRD cystic rats. The authors reported an increased S473-Akt in female *Cy/+* after 9 weeks of ip injections of 0.2 mg/kg rapamycin per day. Interestingly, the opposite effect was observed when the same approach was applied in male *Cy/+* rats, decreasing the S473-Akt activity suggesting a dose-dependent alteration of the S473-Akt regulation. Furthermore, differences in drug application method and treatment duration (gavage, 5 weeks treatment *versus*

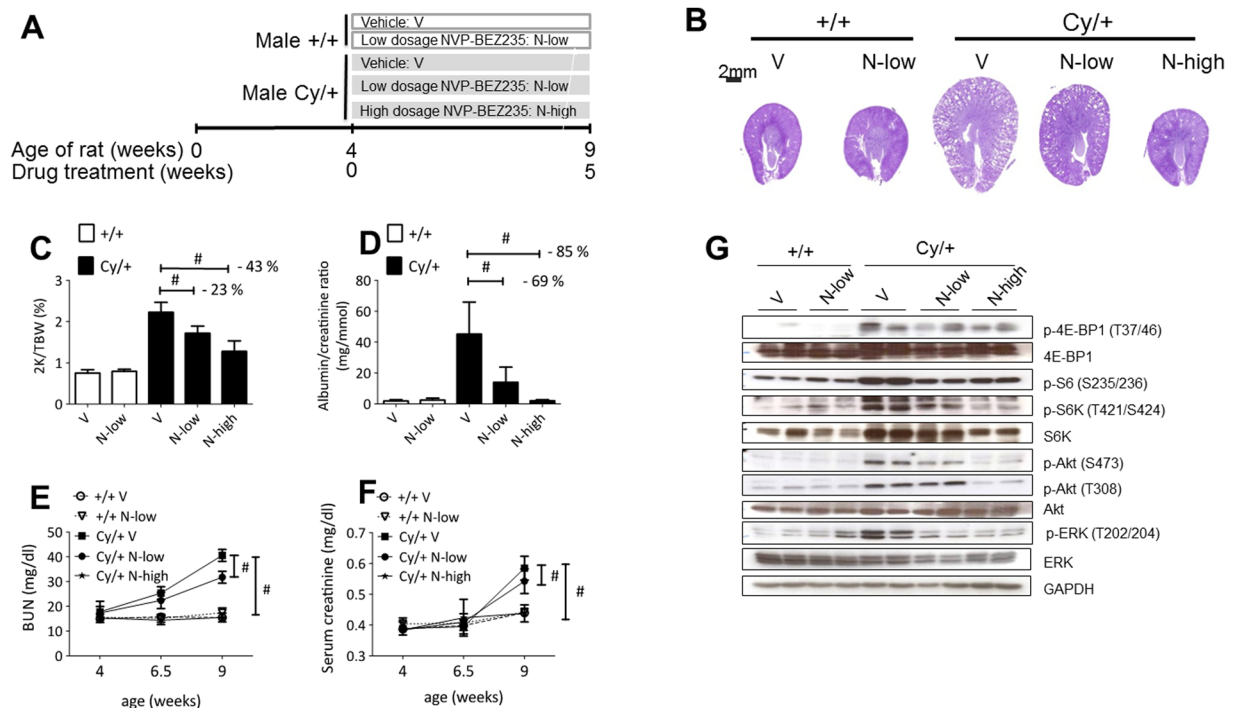


Figure 2. Efficacy of NVP-BEZ235 treatment on Han:SPRD rats renal function. (A) Study design scheme. Dose-dependent effect of NVP-BEZ235 on PKD progression. (B) Representative PAS stained kidney sections of NVP-BEZ235-treated and vehicle-treated Han:SPRD rats. Quantitative analysis of (C) two kidneys to total body weight ratio (2K/TBW), (D) 24 h urine albumin to creatinine ratio, (E) BUN, (F) serum creatinine in Han:SPRD rats are displayed. (G) Western blot analysis of Han:SPRD whole kidney lysates for readouts of mTOR, PI3K/Akt and PI3K/ERK pathways after 5 weeks treatment with NVP-BEZ235-treated and vehicle-treated rat. Representative results of three independent experiments are shown. These are cropped gels and the original gels are presented in Supplementary Fig. 6. * $p < 0.05$, ** $p < 0.01$, # $p < 0.001$ indicated by brackets (mean \pm SD, ANOVA). The number of rat per group is indicated in Supplementary Tables 1 and 2.

ip injection, 9 weeks treatment) may affect fibrosis and Akt expression levels^{15–17}. Our *in vitro* and animal data highlighted the importance of mTOR inhibitors in assessing the effect on pro-proliferative signaling pathways in cystic pre-clinical animal models.

Currently, it is well-known that ADPKD is characterized by complex molecular interactions that contribute to cyst formations and further disease progression¹⁸. Often, due to the lack of appropriate translatability between humans and animal models, there are only a few pathological aspects that can be captured¹⁹. For this reason the initial PKD-associated signaling pathways were further investigated in ADPKD patients enrolled in the SUISE ADPKD study⁵. While polycystic kidney specimens were not available from this trial, peripheral blood mononuclear cells (PBMCs) were isolated from patients before and after treatment with either sirolimus or standard care for 6 months^{20–22}. Among sirolimus treated patients phosphorylation of ribosomal S6 protein was blocked whereas ERK phosphorylation was markedly increased and phospho-Akt was increased in 2 out of the total of 3 sirolimus treated ADPKD patients (Supplementary Fig. 1). Analysis and interpretation of our laboratory data suggested similar effects of mTOR inhibition on pro-proliferative signaling in humans with ADPKD. Therefore, we further investigated the impact of mTOR signaling pathway upon treatment with mTOR inhibitors in Han:SPRD Cy/+ male renal tubular epithelial cells²¹. The set of everolimus, UO126, and perifosine inhibitors provoked triple inhibition of mTOR, ERK and Akt and in the same time considerably more effective loss of cell viability and inhibition of DNA synthesis than any double drug combination (Fig. 1C). Western blot analysis confirmed the effect of each inhibitor on the respective pathways (Fig. 1D).

The suspension of abnormal cyst proliferation and expansion *in vivo* was investigated by administration of NVP-BEZ235 treatment, a dual mTOR/PI3K inhibitor with proven efficacy in various human cancer models^{23–25}. In this analysis, we administrated low-dose (15 mg/kg/day, named N-low group) and high-dose (50 mg/kg/day, named N-high) NVP-BEZ235 to Han:SPRD male rats between 4 and 9 weeks of age (Fig. 2A). Although this treatment reduced the body weight gain, in particular at the higher dose regimen, it had a dramatically positive effect on all aspects of the PKD disease burden: the kidney morphology (evaluated as the two kidneys weight/total body weight ratio, cyst volume, parenchymal fibrosis, and cell proliferation) was similar in NVP-BEZ235-treated PKD and in *wild type* animals (Fig. 2B,C Supplementary Fig. 4A–D and Supplementary Tables 1,2). In addition, renal function (blood urea nitrogen, serum creatinine concentration, urine albumin/creatinine ratio and plasma concentration) were all similar to that recorded in *wild type* animals (Fig. 2D–F and Supplementary Tables 1,2,7). We assessed the urinary proteomic/peptidomic molecular changes in the Han:SPRD rats to explore a potential

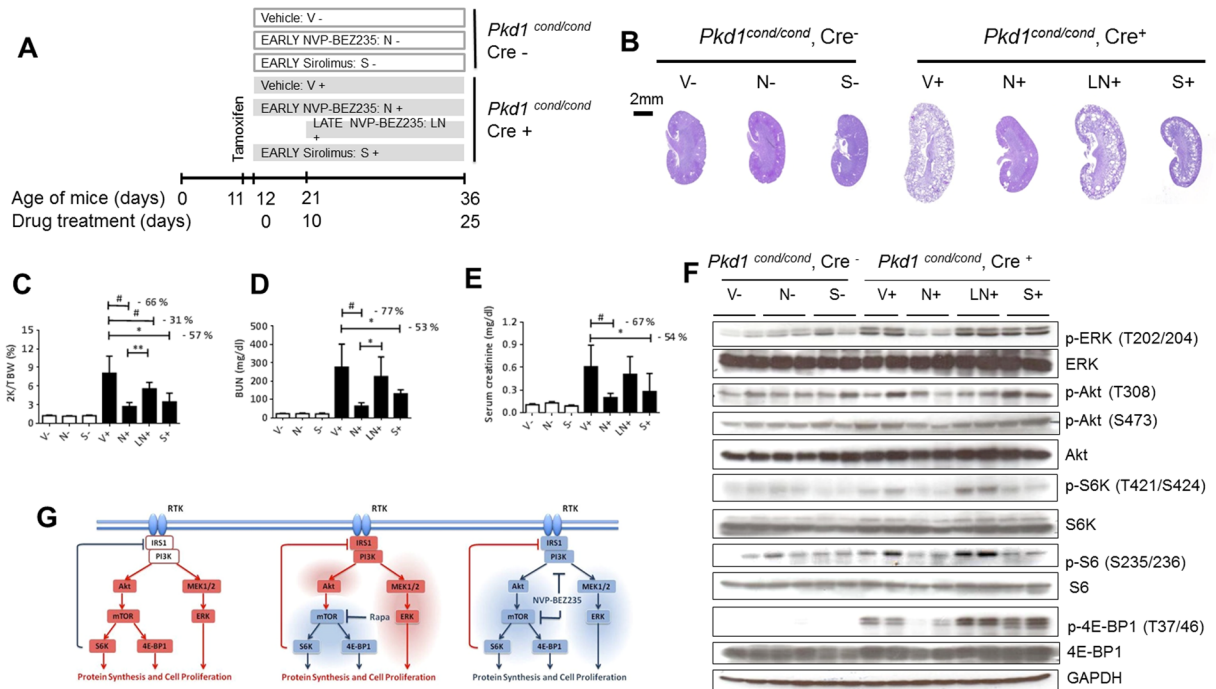


Figure 3. Efficacy of NVP-BEZ235 and sirolimus treatment in *Pkd1* conditional knockout mice. **(A)** Study design scheme. **(B)** Representative PAS stained kidney sections of NVP-BEZ235-treated, sirolimus-treated and vehicle-treated mice. Quantitative analysis of **(C)** two kidneys to total body weight ratio (2K/TBW), **(D)** BUN, **(E)** serum creatinine, * $p < 0.05$, ** $p < 0.01$, *** $p < 0.001$ indicated by brackets (mean \pm SD, ANOVA). The number of mice per group is indicated in Supplementary Tables 4 and 5. **(F)** Whole kidney lysates Western blot analysis of mTOR, PI3K/Akt and PI3K/ERK pathways **(G)** Schematic representation of the pathways examined in the study. mTOR pathway is abnormally activated in polycystic kidneys (left panel). Treatment with mTOR inhibitor results in a hyperactive PI3K-dependent pathway, increasing the signal toward the PI3K/Akt and PI3K/ERK pathway (middle panel). Dual mTOR/PI3K inhibitor NVP-BEZ235 may provide a therapeutic benefit for ADPKD by abrogating the activation of PI3K/Akt and PI3K/ERK pathways and in turn block the mTOR pathway (right panel). Red denotes activated; blue, inhibited. These are cropped gels and original gels are presented in the Supplementary Fig. 6.

biomarker associated with the beneficial effect of the NVP-BEZ235 treatment²⁶. (Supplementary Figure S6 and Supplementary Table 3). None of the animals died during the study and we observed a similar effect on body weight as reported for other mTORC1 inhibitors^{8,27}. Notably, the renal function after 5 weeks of treatment was better in NVP-BEZ235-treated animals compared to everolimus-treated ones (Supplementary Table 4)⁸.

We elucidated the NVP-BEZ235 mode of action by analyzing the mTOR and its dual feedback loop pathway *in vivo*. NVP-BEZ235 blocked the mTOR pathway, as shown by the decrease of phospho-T421/S424-S6K and phospho-S235/236-S6. Expression of phospho-T308-Akt, phospho-S473-Akt and phospho-T202/204-ERK, used to monitor activation of the dual feedback loop, was prevented by the high-dose regimen, whereas the low-dose regimen was already sufficient to reduce the levels of phospho-S473-Akt and phospho-T202/204-ERK (Fig. 2G and Supplementary Fig. 3A). Kidney tissue sections of untreated-Cy/+ rats showed that cysts-lining epithelial cells stained strongly positive for phospho-T202/204-ERK and phospho-S235/236-S6 in the cortex and in the corticomedullary region, whereas *wild type* and NVP-BEZ235-treated animals displayed only a mild and scattered positive staining (Supplementary Fig. 4A). NVP-BEZ235 activates ERK in some cancer cells²⁸ whereas we did not observe an ERK activation in our polycystic kidney models, nor in primary renal tubular epithelial cells (Fig. 2G and Supplementary Fig. 3B)^{25,29,30}. Thus, dual mTOR/PI3K inhibition abrogates the up-regulation of Akt and ERK signaling pathways. Of note, NVP-BEZ235 had no effect on the pro-proliferative pathways, when analyzed in *wild type* treated kidneys, suggesting that the mode of action is specific for ADPKD (Fig. 2L).

To further assess the relevance of dual mTOR and PI3K-dependent pathway inhibition as a therapy for PKD, we compared the efficacy of NVP-BEZ235 and sirolimus in an orthologous ADPKD mouse model with a conditionally inactivated *Pkd1* gene³¹. Firstly, we induced cystogenesis by tamoxifen intraperitoneal (ip) injection into pups at postnatal day 11, then deterioration of the kidney function occurred over 4 to 6 weeks³². We assessed the efficacy of NVP-BEZ235 for two different treatment initiation time points: At an early disease state with 6 mg/kg dosage before weaning between day 12 and day 35 and at the same time points with 9 mg/kg after weaning (N+ group). Over the same time period, sirolimus with 3 mg/kg dosage (S+ group) was also applied. The late disease stage drug administration was evaluated between day 21 and 35 with the ip method of injection and dosage of 9 mg/kg NVP-BEZ235 (LN+ group) (Fig. 3A). Our preclinical results showed a marked beneficial effect at early disease stage mirrored by reducing kidney volume and preserving further cysts enlargement (Fig. 3B,C). Furthermore early treatment preserved body weight (Supplementary Fig. 3C); prevented kidney function decline

(blood urea nitrogen levels (Fig. 3D) and serum creatinine levels (Fig. E)): inhibited cytogenesis (Supplementary Fig. 5B), fibrogenesis (Supplementary Fig. 5C) and cell proliferation (Supplementary Fig. 5D). Sirolimus (S+ group) was less efficient than NVP-BEZ235 (N+ group) with respect to cystogenesis, renal function and proliferation (Fig. 3B–E and Supplementary Fig. 5B–D). Western blot analysis displayed reduced expression of phospho-S6K, phospho-S6 and phospho-4EBP and no up-regulation phospho-ERK and phospho-Akt during early stage PKD (N+ group) whereas sirolimus (S+ group) triggered Akt activation (Fig. 3F and Supplementary Fig. 3). Late NVP-BEZ235-treated mice (LN+ group) exhibited renal function decline among all three treatment groups (Fig. 3B–E), and Western blot analysis indicated increased gene expression of phospho-T202/204-ERK, phospho-T421/S424-S6K, and phospho-S235/236-S6 (Supplementary Fig. 5A and Supplementary Tables 5,6).

Ren and his colleagues investigated safety and efficacy of NVP-BEZ235 in PCK rats, an established autosomal recessive polycystic kidney (ARPKD) model. The NVP-BEZ235 had no beneficial effect on cystogenesis in the ARPKD rodent model³³. In another study, Pollizi and the colleagues have shown that NVP-BEZ235 and everolimus had equivalent effects in suppressing the development of cystadenomas in a TSC2 mouse model³⁴. In clinical practice, assessment of safety and efficiency of NVP-BEZ235 in 20 patients with locally advanced or metastatic transitional cell carcinoma (TCC) after failure of platinum-based therapy showed only moderate beneficial effect and severe drug-related complications in the majority of the patients³⁵. We assume that even greater toxicity would be observed in humans required for ADPKD given the longer term dosing. Therefore, careful risk stratification is of utmost importance to identify patients eligible for treatments to balance therapeutic efficacy and possible adverse effects.

Our signaling pathway analysis after NVP-BEZ235 treatment suggests a feedback loop. Indeed, a recent study has demonstrated that there is a new feedback loop compensatory activation of Rictor and S473-Akt via FoxO-mediated upregulation after NVP-BEZ235 treatment which can be used as a novel therapeutic target in human renal carcinoma cells³⁶. Another study has shown that NVP-BEZ235 is a potential inhibitor of ataxia telangiectasia mutated (ATM) and DNA-dependent protein kinase (DNA-PK), which are unexplored but may implicate the DNA double strand break (DNA-DSB) repair pathways in PKD^{37–39}.

Our findings that sirolimus treatment increased renal S473-Akt level in the orthologous ADPKD mouse model was not observed in the study of Shillingford and colleagues. The difference could be associated with the PKD1^{cond/cond};Nestin^{Cre} mice used by Shillingford. In this mouse model renal cysts arise predominantly from the collecting duct and distal tubules whereas in our PKD1^{cond/cond};Tamoxifen-Cre+ mice cysts develop in all nephron segments and renal dysfunction occurs over 4 to 6 weeks. Future experimental studies using a slow progressive disease model and PKD1^{cond/cond};Nestin^{Cre} model is needed to further elucidate the effect of NVP-BEZ235 on the signaling pathway associated with cystogenesis and cyst progression^{6,32}.

Our study has to be interpreted in the context of the study design. Firstly, the experiments in the animal models are performed in relatively small group sizes. Secondly, only males were used for the Han:SPRD rats due to the different rate of disease progression in male and female rats. Thirdly, the effect of NVP-BEZ235 at high doses on the body weight of Han:SPRD rat suggests toxicity and thus warrants careful consideration before applying this drug in clinical trials. Our pre-clinical data indicated the beneficial effect of the dual mTOR/PI3K inhibitor NVP-BEZ235 and highlighted the need for well-designed clinical trials to explore NVP-BEZ235 as a potential treatment in ADPKD patients.

Conclusion

In conclusion, blockage of the mTOR pathway, by using mTOR inhibitors, triggers up-regulation of pro-proliferative PI3K-dependent pathways, either through the PI3K/Akt or PI3K/ERK pathway in PKD. Dual mTOR/PI3K inhibition specifically prevents the activation of these feedback loops and (Fig. 3G), when applied in early stage disease, this treatment normalizes the renal function and the morphology of ADPKD non-orthologous rat and orthologous mice models.

Methods

The protocols and methods used in this study were in accordance with the EU Directive 2010/63/EU-On the protection of animal for experimental and other scientific purposes. All standards, international convention and declaration were supervised by the European Group on Ethics and Protection of Animals.

Experimental animals and study design. *Han:SPRD rat.* The Han:SPRD rat colony was established in our animal facility from a litter, which was obtained from the Rat Resource and Research Center (Columbia, MO). Heterozygous cystic (Cy/+) and wild-type (+/+) male rats were used in this study. Figure 2A display the rat study set up: we applied by gavage NVP-BEZ235 (Novartis) at low-dose (15 mg/kg/day), high-dose (50 mg/kg/day) and vehicle solution (90% PEG300 and 10% 1-mehtyl-2-pyrrolidinone, Sigma-Aldrich) from 4 to 9 weeks of age. Blood was collected at 4, 6.5 and 9 weeks of age for determination of serum creatinine and BUN levels. 24 h urine samples were collected in metabolic cages one day before the rats were killed. We applied by gavage everolimus (E, 3 mg/kg/day) and vehicle solution (V) from 4 to 16 weeks of age. Rats were anesthetized with isoflurane and kidneys were harvested for further analysis.

Pkd1 conditional knockout mouse. Professor G.G Germino supplied the Pkd1 conditional knockout mouse. We induced Cre recombinase activity by intraperitoneal injection of tamoxifen (1.25 mg/10 g, dissolved in corn oil (Sigma-Aldrich) at day 11 of age into pups. Figure 3A display the mice study set up: The mice were randomly allocated to seven groups; Pkd1^{cond/cond}, Cre + vehicle (V+), Pkd1^{cond/cond}, Cre+ early-phase NVP-BEZ235 (N+), Pkd1^{cond/cond}, Cre+ late-phase NVP-BEZ235 (LN+), Pkd1^{cond/cond}, Cre+ early-phase sirolimus (S+), Pkd1^{cond/cond}, Cre- vehicle (V-), Pkd1^{cond/cond}, Cre- early-phase NVPBEZ235(N-), and Pkd1^{cond/cond}, Cre- early-phase sirolimus (S-). For the N+ and Ngroups, animals were treated with 6 mg/kg/day NVP-BEZ235

from day 12 to day 20, and later with 9 mg/kg/day until day 35. For the S+ and S− groups, 3 mg/kg/day sirolimus was administered from day 12 to day 35. For the LN+ group, mice were

treated with 9 mg/kg/day NVP-BEZ235 from day 21 to day 35. NVP-BEZ235, sirolimus and vehicle solutions were administered by intraperitoneal injections. 24 h urine samples were collected by metabolic cage at day 35. Mice were anesthetized with isoflurane at day 36, and blood was obtained by cardiac puncture for determination of serum creatinine and BUN levels and kidneys were harvested for further analysis.

Biochemical analysis. Rat and mice serum creatinine and BUN levels were detected with UniCel[®] Dx C 800 Synchron[®] Clinical (Zurich Integrative Rodent Physiology). The GenWay Albumin Elisa Kits for rat were used for rat urine albumin concentration measurement, according to the manufacturer's protocol.

Proteomic analysis. PKD rat urine aliquots were thawed immediately before use and 150 µl were mixed with 150 µl solution containing 2 M urea, 10 mM NH₄OH and 0.02% SDS. Subsequently, aliquots were filtered with Centriscart ultracentrifugation filters (20 kDa MWCO, Sartorius, Goettingen, Germany) to remove the higher molecular weight proteins. Obtained filtrate was desalted using a NAP 5 gel filtration column (GE Healthcare Bio Science, Uppsala, Sweden) to remove urea and electrolytes. Samples were lyophilized and stored on 4 °C. Shortly before CE-MS analysis, the aliquots were re-suspended in 10 µl HPLC grade H₂O. CE-MS technology was performed using P/ACE MDQ capillary electrophoresis system (Beckman Coulter, Fullerton, CA), on-line couple to a Micro-TOF MS (Bruker Daltonic, Bremen, Germany). Spectra were accumulated every 3 s over m/z range of 350–3000 Da. Details of the CE-MS technology has been described previously⁴⁰. Proteomic data was further processed by MosaVisu software package in order to deconvolve mass spectral ion peaks representing identical molecules at different charge states into single masses. Normalization of migration time and ion signal intensity (amplitude) was achieved by using internal endogenous peptide standards for biomarker quantification. Based on this approach using “housekeeping” peptides, calculation of the relative abundance allows both correction of analytical variance and correction for different dilution levels of individual urine samples. All detected polypeptides, characterized by their molecular mass (kDa), CE-migration time (min) and ion signal intensity, were matched and annotated by usage of Microsoft SQL database. Peptide marker panel was established using support vector machine (SVM)-based MosaCluster software package⁴¹. The reported p-values of the identified potential peptide markers were calculated with Wilcoxon Rank Sum test followed by adjustment of multiple testing with the method described by Benjamini and Hochberg⁴². Peptides detected with frequency of ≥90% in at least one of the animal groups were considered for statistical analysis.

To obtain sequence informations, urine samples were analyzed on a Dionex Ultimate 3000 RSLC nano flow system (Dionex, Camberly UK) couple to an Orbitrap Velos FTMS (Thermo Fisher, Bremen, Germany). The fragmentation method was HCD at 35% collision energy. FTMS analyzer was selected with 60 000 resolution for MS1 and 7500 resolution for MS2. Peptides and proteins were searched against UniProt rat database and identified with SEQUEST spectral algorithm (Thermo), without any enzyme specificity. Precursor mass tolerance and fragment mass tolerance were 10 ppm and 0.05 Da, respectively. No fixed modification was selected and oxidation of methionine and proline were set up as variable modifications. High confidence peptides with Xcorr ≥1.9 and rank 1 were accepted as most valid for identification of the peptide markers⁴³. Mass deviation was set below ±80 ppm.

Statistics. Data are presented as mean ± SD. Statistical differences between treatment groups were performed by the unpaired two-tailed *t*-test using GraphPad Prism version 4.0 (GraphPad). *P* < 0.05 was considered to be statistically significant.

Study approval. The study was approved and ruled under animal license number 22/2010 obtained from Zürich Veterinary Office.

Availability of data and materials. The raw datasets used and/or analyzed during the current study are available from the corresponding author on reasonable request.

References

- Harris, P. C. & Torres, V. E. Polycystic kidney disease. *Annu Rev Med* **60**, 321–337 (2009).
- Boletta, A. Emerging evidence of a link between the polycystins and the mTOR pathways. *Pathogenetics* **2**(1), 6 (2009).
- Bonnet, C. S. *et al.* Defects in cell polarity underlie TSC and ADPKD-associated cystogenesis. *Hum Mol Genet* **18**(12), 2166–2176 (2009).
- Novalic, Z. *et al.* Dose-dependent effects of sirolimus on mTOR signaling and polycystic kidney disease. *J Am Soc Nephrol* **23**(5), 842–853 (2012).
- Serra, A. L. *et al.* Sirolimus and kidney growth in autosomal dominant polycystic kidney disease. *N Engl J Med* **363**(9), 820–829 (2010).
- Shillingford, J. M., Piontek, K. B., Germino, G. G. & Weimbs, T. Rapamycin ameliorates PKD resulting from conditional inactivation of Pkd1. *J Am Soc Nephrol* **21**(3), 489–497 (2010).
- Walz, G. & Budde, K. *et al.* Everolimus in patients with autosomal dominant polycystic kidney disease. *N Engl J Med* **363**(9), 830–840 (2010).
- Wu, M. *et al.* Everolimus retards cyst growth and preserves kidney function in a rodent model for polycystic kidney disease. *Kidney Blood Press Res* **30**(4), 253–259 (2007).
- Carracedo, A. *et al.* Inhibition of mTORC1 leads to MAPK pathway activation through a PI3K-dependent feedback loop in human cancer. *J Clin Invest* **118**(9), 3065–3074 (2008).
- Svejda, B. *et al.* Limitations in small intestinal neuroendocrine tumor therapy by mTOR kinase inhibition reflect growth factor-mediated PI3K feedback loop activation via ERK1/2 and AKT. *Cancer* **117**(18), 4141–4154 (2011).
- Veilleux, A., Houde, V. P., Bellmann, K. & Marette, A. Chronic inhibition of the mTORC1/S6K1 pathway increases insulin-induced PI3K activity but inhibits Akt2 and glucose transport stimulation in 3T3-L1 adipocytes. *Mol Endocrinol* **24**(4), 766–778 (2010).
- Zitzmann, K. *et al.* Compensatory activation of Akt in response to mTOR and Raf inhibitors - a rationale for dual-targeted therapy approaches in neuroendocrine tumor disease. *Cancer Lett* **295**(1), 100–109 (2010).

13. Gretz, N. *et al.* Rat models of autosomal dominant polycystic kidney disease. *Nephrol Dial Transplant* **11**(Suppl 6), 46–51 (1996).
14. Wu, M. *et al.* Pulse mTOR inhibitor treatment effectively controls cyst growth but leads to severe parenchymal and glomerular hypertrophy in rat polycystic kidney disease. *Am J Physiol Renal Physiol* **297**(6), F1597–F1605 (2009).
15. Kim, H. W. *et al.* Cyclic AMP controls mTOR through regulation of the dynamic interaction between Rheb and phosphodiesterase 4D. *Mol Cell Biol* **30**(22), 5406–5420 (2010).
16. Lu, D. & Insel, P. A. Cellular mechanisms of tissue fibrosis. 6. Purinergic signaling and response in fibroblasts and tissue fibrosis. *Am J Physiol Cell Physiol* **306**(9), C779–C788 (2014).
17. Schinner, E., Wetzl, V. & Schlossmann, J. Cyclic nucleotide signalling in kidney fibrosis. *Int J Mol Sci* **16**(2), 2320–2351 (2015).
18. Pejchinovski, M. *et al.* Urinary peptidome analysis predicts the risk of end stage renal disease and reveals proteolytic pathways involved in autosomal dominant polycystic kidney disease progression. *Nephrol Dial Transplant* **32**(3), 487–497 (2017).
19. Klein, J. *et al.* Urinary peptidomics provides a noninvasive humanized readout of diabetic nephropathy in mice. *Kidney Int* **90**(5), 1045–1055 (2016).
20. Berk, L. *et al.* Analysis of the pharmacodynamic activity of the mTOR inhibitor ridaforolimus (AP23573, MK-8669) in a phase 1 clinical trial. *Cancer Chemother Pharmacol* **69**(5), 1369–1377 (2012).
21. Canaud, G. *et al.* Therapeutic mTOR inhibition in autosomal dominant polycystic kidney disease: What is the appropriate serum level? *Am J Transplant* **10**(7), 1701–1706 (2010).
22. Tanaka, C. *et al.* Identifying optimal biologic doses of everolimus (RAD001) in patients with cancer based on the modeling of preclinical and clinical pharmacokinetic and pharmacodynamic data. *J Clin Oncol* **26**(10), 1596–1602 (2008).
23. Brachmann, S. M. *et al.* Specific apoptosis induction by the dual PI3K/mTOR inhibitor NVP-BEZ235 in HER2 amplified and PIK3CA mutant breast cancer cells. *Proc Natl Acad Sci USA* **106**(52), 22299–22304 (2009).
24. Engelman, J. A. *et al.* Effective use of PI3K and MEK inhibitors to treat mutant Kras G12D and PIK3CA H1047R murine lung cancers. *Nat Med* **14**(12), 1351–1356 (2008).
25. Roccaro, A. M. *et al.* Dual targeting of the PI3K/Akt/mTOR pathway as an antitumor strategy in Waldenstrom macroglobulinemia. *Blood* **115**(3), 559–569 (2010).
26. Mischak, H. *et al.* Capillary electrophoresis-mass spectrometry as a powerful tool in biomarker discovery and clinical diagnosis: An update of recent developments. *Mass Spectrom Rev* **28**(5), 703–724 (2009).
27. Belibi, F., Ravichandran, K., Zafar, I., He, Z. & Edelstein, C. L. mTORC1/2 and rapamycin in female Han:SPRD rats with polycystic kidney disease. *Am J Physiol Renal Physiol* **300**(1), F236–F244 (2011).
28. Moon, d. G. *et al.* NVP-BEZ235, a dual PI3K/mTOR inhibitor synergistically potentiates the antitumor effects of cisplatin in bladder cancer cells. *Int J Oncol* **45**(3), 1027–1035 (2014).
29. Jin, N., Jiang, T., Rosen, D. M., Nelkin, B. D. & Ball, D. W. Synergistic action of a RAF inhibitor and a dual PI3K/mTOR inhibitor in thyroid cancer. *Clin Cancer Res* **17**(20), 6482–6489 (2011).
30. Sunayama, J. *et al.* Crosstalk between the PI3K/mTOR and MEK/ERK pathways involved in the maintenance of self-renewal and tumorigenicity of glioblastoma stem-like cells. *Stem Cells* **28**(11), 1930–1939 (2010).
31. Piontek, K. B. *et al.* A functional floxed allele of Pkd1 that can be conditionally inactivated *in vivo*. *J Am Soc Nephrol* **15**(12), 3035–3043 (2004).
32. Piontek, K., Menezes, L. F., Garcia-Gonzalez, M. A., Huso, D. L. & Germino, G. G. A critical developmental switch defines the kinetics of kidney cyst formation after loss of Pkd1. *Nat Med* **13**(12), 1490–1495 (2007).
33. Ren, X. S. *et al.* Activation of the PI3K/mTOR pathway is involved in cystic proliferation of cholangiocytes of the PCK rat. *PLoS ONE* **9**(1), e87660 (2014).
34. Pollizzi, K., Malinowska-Kolodziej, I., Stumm, M., Lane, H. & Kwiatkowski, D. Equivalent benefit of mTORC1 blockade and combined PI3K-mTOR blockade in a mouse model of tuberous sclerosis. *Mol Cancer* **8**, 38 (2009).
35. Seront, E. *et al.* Phase II study of dual phosphoinositol-3-kinase (PI3K) and mammalian target of rapamycin (mTOR) inhibitor BEZ235 in patients with locally advanced or metastatic transitional cell carcinoma. *BJU Int* **118**(3), 408–415 (2016).
36. Lin, A. *et al.* FoxO transcription factors promote AKT Ser473 phosphorylation and renal tumor growth in response to pharmacologic inhibition of the PI3K-AKT pathway. *Cancer Res* **74**(6), 1682–1693 (2014).
37. Chen, Y. H. *et al.* Dual phosphoinositide 3-kinase/mammalian target of rapamycin inhibitor is an effective radiosensitizer for colorectal cancer. *Cancer Lett* **357**(2), 582–590 (2015).
38. Gil del Alcazar, C. R. *et al.* Inhibition of DNA double-strand break repair by the dual PI3K/mTOR inhibitor NVP-BEZ235 as a strategy for radiosensitization of glioblastoma. *Clin Cancer Res* **20**(5), 1235–1248 (2014).
39. Mukherjee, B. *et al.* The dual PI3K/mTOR inhibitor NVP-BEZ235 is a potent inhibitor of ATM- and DNA-PKCs-mediated DNA damage responses. *Neoplasia* **14**(1), 34–43 (2012).
40. Novak, J., Weissinger, E. M., Schanstra, J. P. & Dominiczak, A. F. Capillary electrophoresis-mass spectrometry as a powerful tool in biomarker discovery and clinical diagnosis: An update of recent developments. *Mass Spectrom Rev* **28**(5), 703–724 (2009).
41. Mischak, H. *et al.* Comprehensive human urine standards for comparability and standardization in clinical proteome analysis. *Proteomics Clin Appl* **4**(4), 464–478 (2010).
42. Benjamini, Y. & Hochberg, Y. Controlling the false discovery rate: a practical and powerful approach to multiple testing. *J Royal Stat Soc B (Methodological)* **57**(1), 125–133 (1995).
43. Pejchinovski, M. *et al.* Comparison of higher energy collisional dissociation and collision-induced dissociation MS/MS sequencing methods for identification of naturally occurring peptides in human urine. *Proteomics Clin Appl* **9**(5-6), 531–542 (2015).

Acknowledgements

This work was supported by grants from the Swiss National Science Foundation (310030–132597 to AS), the NKF of Maryland (R37DK48006, R01DK095036 to TW), the TranCYST (FP7-PEOPLE-MCA-ITN no. 317246 to AS and HM) and the Chinese Government Scholarship (YL). The funders had no role in study design, data collection and analysis, decision to publish, or preparation of the manuscript. We thank Gregory G. Germino for supplying *Pkd1* conditional knockout mice, Michel S. Maira for analyzing plasma concentration of NVP-BEZ235 in rats, Novartis AG for providing NVP-BEZ235, Hongbo Zhang for breeding the *Pkd1* conditional knockout mice, Charlotte Burger for technical assistance, Julien Weber for blood and urine samples analysis. We thank Ian Frew and Johannes Loffing for helpful discussions and critical manuscript reading.

Author Contributions

Y.L. designed and performed the experiments, analyzed data and wrote the manuscript. M.P. performed the proteomic analysis and contributed in writing the manuscript. X.W. and X.F. performed the *in vivo* experiments with NVP-BEZ235 treatment. D.C., A.A., J.S., W.M. and H.M. designed the studies and discussed results. T.J.W. supplied the *Pkd1* conditional knockout mice. A.L.S. designed the experiments and studies, supervised the work and wrote the manuscript.

Additional Information

Supplementary information accompanies this paper at <https://doi.org/10.1038/s41598-018-22938-x>.

Competing Interests: H.M. is founder and co-owner of Mosaiques Diagnostics GmbH, who developed CE-MS technology. M.P. and J.S. are employees of Mosaiques Diagnostics GmbH.

Publisher's note: Springer Nature remains neutral with regard to jurisdictional claims in published maps and institutional affiliations.



Open Access This article is licensed under a Creative Commons Attribution 4.0 International License, which permits use, sharing, adaptation, distribution and reproduction in any medium or format, as long as you give appropriate credit to the original author(s) and the source, provide a link to the Creative Commons license, and indicate if changes were made. The images or other third party material in this article are included in the article's Creative Commons license, unless indicated otherwise in a credit line to the material. If material is not included in the article's Creative Commons license and your intended use is not permitted by statutory regulation or exceeds the permitted use, you will need to obtain permission directly from the copyright holder. To view a copy of this license, visit <http://creativecommons.org/licenses/by/4.0/>.

© The Author(s) 2018